

## DESIGN OF THE CATHODE STALK FOR THE LCLS-II-HE LOW EMITTANCE INJECTOR\*

T. Konomi<sup>†</sup>, W. Hartung, S. Kim, S. Miller, D. Morris, J. Popielarski, K. Saito, A. Taylor, T. Xu  
Facility for Rare Isotope Beams, Michigan State University, East Lansing, MI, USA

M. Kelly, T. Petersen, Argonne National Laboratory, Lemont, IL, USA

C. Adolphsen, J. Lewellen, SLAC National Accelerator Laboratory, Menlo Park, CA, USA

S. Gatzmanga, P. Murcek, R. Xiang, Helmholtz Zentrum Dresden Rossendorf, Dresden, Germany

### Abstract

Superconducting radio-frequency (SRF) electron guns are attractive for delivery of beams at a high bunch repetition rate but moderate accelerating field. An SRF gun is the most suitable injector for the high-energy upgrade of the Linac Coherent Light Source (LCLS II-HE), which will produce high-energy X-rays at high repetition rate. An SRF gun is being developed for LCLS-II HE as a collaborative effort by FRIB, HZDR, ANL, and SLAC. The cavity operating frequency is 185.7 MHz and the target accelerating field at the photocathode is 30 MV/m. The photocathode is replaceable. The cathode is held by a fixture (“cathode stalk”) which is designed for thermal isolation and particle-free cathode exchange. The stalk must allow for precise alignment of the cathode position, cryogenic or room-temperature cathode operating temperature, and DC bias to inhibit multipacting. We are planning a test of the stalk to confirm that the design meets the requirements for RF power dissipation and biasing.

### INTRODUCTION

XFELs are powerful tools for revealing structural dynamics at the atomic scale. The LCLS-II-HE will achieve a hard X-ray of 13 keV by doubling the beam energy to 8 GeV from that in LCLS-II. Furthermore, the photon energy of LCLS-II-HE can reach 20 keV by factor of two reduction in the electron source emittance [1].

The development of a low frequency quarter-wave resonator (QWR) SRF gun was proposed to achieve a low emittance beam. The advantage of such a gun is that it can provide a quasi-DC field in the accelerating gap and operate at 4K. As with other SRF guns, an ultra-low vacuum level can be achieved, which allows a wider range of photocathodes to be used.

One of the critical parameters for a high-brightness electron source is the cathode gradient. The goal of the gun cavity development is to demonstrate stable CW operation with a cathode gradient of at least 30 MV/m.

### CATHODE STALK DESIGN

The cavity frequency was selected to be 185.7 MHz, which is one-seventh of the 1300 MHz LCLS-II linac frequency. The cavity shape was designed to mitigate multipacting and was evolved from the WIFEL design [2]. The cathode and the cathode stalk use components employed in the SRF gun at HZDR [3].

<sup>†</sup> konomi@frib.msu.edu

There are four main requirements for the cathode stalk. One is precise alignment control of the cathode position. If the cathode position is off-centre, the radial RF field on the cathode will be biased and emittance growth will occur. This growth is difficult to recover with the beam optics downstream of the SRF gun. Second requirement is that it can be biased up to 5kV DC to inhibit multipacting in the coaxial structure of the cathode and cathode stalk. The third requirement is that the temperature of the cathode can be changed if needed, which can improve photocathode performance. The fourth requirement is particle free cathode exchange to prevent field emission from contamination.

The cathode stalk assembly is shown in Fig. 1. The cathode port of the cavity is connected to the bellows flange of the cathode stalk. The tube of the cathode stalk is electrically isolated from the bellows by a ceramic ring. The head of the tube is made of copper and will be cooled by a pipe externally connected to a helium gas supply of either 300 K or 55 K. The tube body is made of stainless steel that is copper/gold plated on the outside to reduce RF loss and thermal emissivity. The cathode holder is conduction cooled through the contact surface with the tube head. The DC bias is connected to a cooling pipe that is electrically isolated using a ceramic break. Three manipulators will be used to adjust the cathode position. These extend to the outside of the cryomodule. The insertion arm for cathode exchange includes four segmented electrodes that are used to sense its transverse location. The cathode holder is inserted into a cone-shaped socket in the cathode head and held in place by a spring.

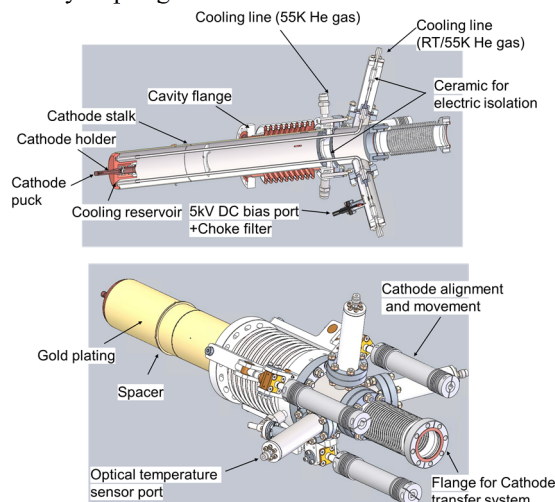


Figure 1: Cathode Stalk assembly.

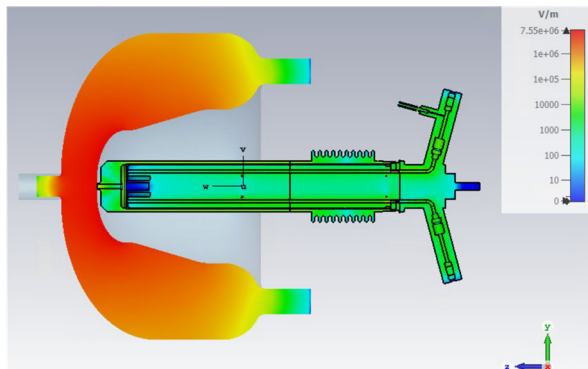
## CAVITY WITH CATHODE STALK

Figure 2 shows a simulation of the stalk electromagnetic field profile and Table 1 lists the gun parameters. Figure 3 shows the change of coupling and cavity frequency when the cathode tip position is moved forward or backward on the beam axis. The coupling between the cavity and the cathode was evaluated assuming a simple coaxial waveguide stalk with a matched load instead of the stalk assembly (with stalk installed, only 17 W is dissipated in it as nearly all of the coupled power is reflected back to the cavity). The coupling simulation shows that a change in cathode tip position of 1 mm increases or decreases the RF power by a factor of about two. The change of cavity frequency is not linear. It can be used to confirm the cathode position. Since the coupling to the cavity is strong, the RF loss in the cathode stalk should be evaluated precisely. Some of the RF leaks into the interior of the cathode holder in part due to the coaxial like structures created by the cooling lines. A choke filter will be connected to the DC bias port to prevent RF leakage from it. Given the complexity of the stalk assembly, there will be an RF/DC test of it to confirm that no unexpected RF heating, multipacting or DC breakdown occurs.

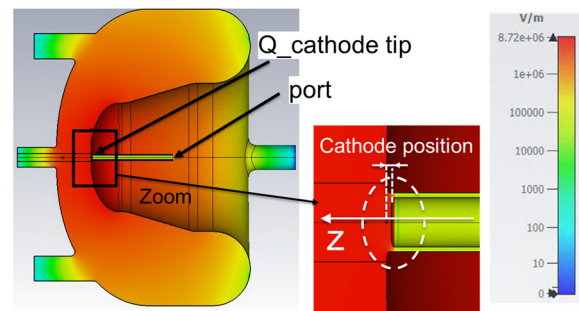
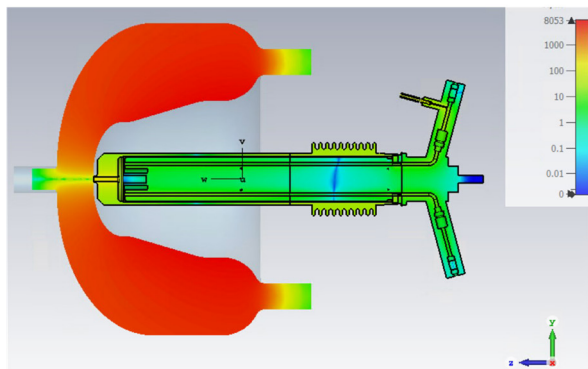
Table 1: RF Parameters of Gun Cavity with Cathode Stalk

Parameters	Value
RF frequency	185.7 MHz
Quality factor at 4.4 K	$6.9 \times 10^8$
Gradient on cathode	30 MV/m
Wall loss on Nb cavity	19.5 W
Wall loss in cathode stalk	17.0 W
Surface peak magnetic field ( $B_{\text{peak}}$ )	53.0 mT
Surface peak electric field ( $E_{\text{peak}}$ )	33.7 MV/m
$E_{\text{peak}}/B_{\text{peak}}$	0.636 (MV/m)/mT
Gap voltage	1.81 MV
Accelerating voltage ( $\beta=1$ )	1.80 MV

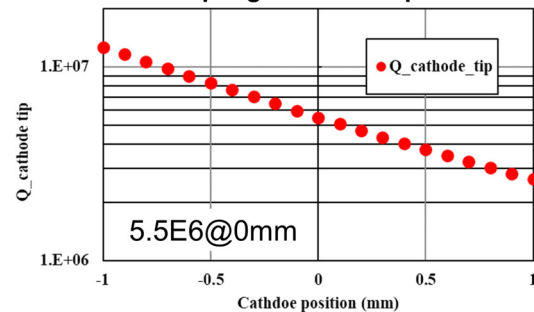
### E-field



### H-field



### Coupling vs cathode position



### Frequency vs cathode position

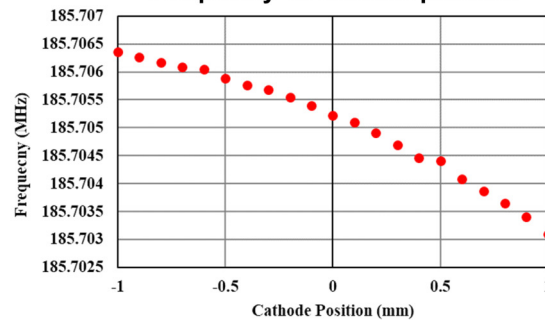


Figure 2: RF electric and magnetic field map of the QWR cavity with cathode stalk.

Figure 3: Coupling and frequency dependence on cathode position.

The cathode stalk is isolated by a ceramic ring. The structure around it is complicated and a relatively high electric field is generated on the ceramic surface. The structure near the ceramic insulation is shown in Fig. 4. The electric field is enhanced by the vacuum gap and the maximum field on the ceramic surface is about 15 MV/m. This value is close to the flashover voltage so it is important that

the DC leakage current be measured during the cathode stalk RF/DC test.

### Model around ceramic support

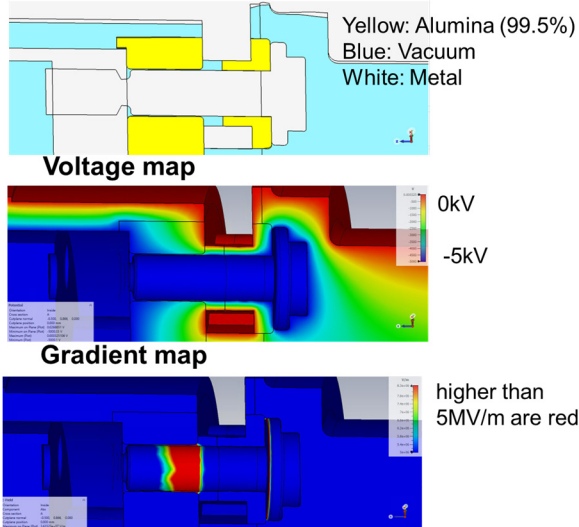


Figure 4: DC field map around the ceramic isolator with a 5 kV bias voltage.

## CATHODE STALK RF/DC TEST

The cathode stalk test will be performed by attaching a 185.7 MHz resonator to the tip of the cathode as shown in Fig. 5. The cathode stalk is connected to the outer conductor of the resonator. The other side of the resonator has an RF input port. This assembly is inserted to a vacuum chamber for thermal isolation. The cathode stalk and the outer conductor have slits at various locations, and the entire cathode stalk is evacuated by a pump connected to the vacuum chamber.

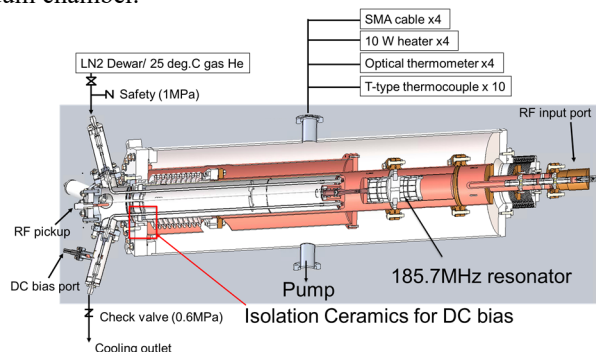


Figure 5: Setup for the cathode stalk RF/DC test.

RF monitor cables and heaters are inserted from the opposite side of the vacuum port. The RF monitor cables are connected to a SMA antenna along the outer conductor and will be used to monitor the RF field distribution. Figure 6 shows the RF field map in the RF/DC test setup. The quality factor of the RF/DC test setup is about 1300 and the input power needs to be at least 43 W to generate the same field levels as will be present when operated in the SRF gun. The cathode will be cooled as during actual gun operation, but liquid nitrogen will be used instead of 55 K helium gas for the cryogenic temperature test.

One of the main objectives of the RF/DC test is to confirm that there is no unexpected RF heating. Each component of the cathode stalk will be measured using local heaters, thermocouples, and optical thermometers in advance of RF operation. This heater test can confirm that the cathode puck can be sufficiently cooled. The cathode puck is cooled through the cathode holder. The cooling path contains a contact thermal resistance at two locations. The temperature of the cathode puck will increase significantly if the surface contact is insufficient.

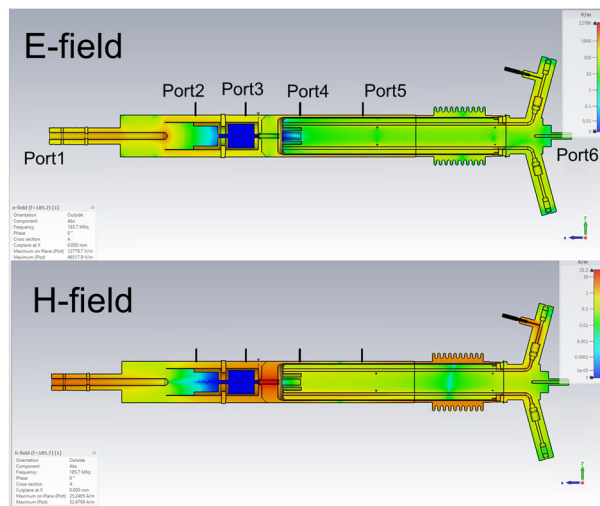


Figure 6: RF field map in the stalk RF/DC test setup.

## SUMMARY

The coupling of the cathode to the cavity is high, about  $5.5 \times 10^6$ , but the RF loss in the cathode stalk is about 17 W. Since RF leaks into the inside of the cathode holder, multipacting is a concern. Also, the surface DC field at the ceramic break is high (15 MV/m). To verify performance, we will build stalk test setup and do a DC bias test, an RF test and measure the thermal profile at room temperature and liquid nitrogen temperature (77 K).

## ACKNOWLEDGEMENTS

This work supported by the Department of Energy Contract DE-AC02-76SF00515.

## REFERENCES

- [1] J. W. Lewellen *et al.*, "Status of the SLAC/MSU SRF Gun Development Project", presented at the NAPAC'22, Albuquerque, New Mexico, USA, Aug. 2022, paper WEPA03, this conference.
- [2] S. H. Kim *et al.*, "Design of a 185.7 MHz Superconducting RF Photoinjector Quarter-Wave Resonator for the LCLS-II-HE Low Emittance Injector", presented at the NAPAC'22, Albuquerque, New Mexico, USA, Aug. 2022, paper MOPA85, this conference.
- [3] J. Teichert *et al.*, "Successful user operation of a superconducting radio-frequency photoelectron gun with Mg cathodes", *Phys. Rev. Accel. Beams*, vol. 24, p. 033401, 2021. doi:10.1103/PhysRevAccelBeams.24.033401